Available online at www.sciencedirect.com
SCIENCE DIRECT
ELSEVIER
European Journal of Mechanics B/Fluids 23 (2004) 851–859
EUROPEAN JOURNAL OF MECHANICS B/FLUIDS

Stability of Bödewadt–Hartmann layers ☆

P. Moresco *, T. Alboussière

Department of Engineering, University of Cambridge, Trumpington Street, Cambridge CB2 1PZ, UK

Received 16 September 2003; received in revised form 16 March 2004; accepted 2 April 2004

Available online 12 May 2004

Abstract

The linear stability of the combined Hartmann and Bödewadt boundary layers was studied for a wide range of values of the Elsasser number Λ (the ratio between the Lorentz forces and inertial effects). It was found that the instability modes originating from rotational effects present the lowest critical Reynolds numbers even at high Λ, showing the importance that three-dimensional effects can have in the stability of the Hartmann layer. The results are discussed in the light of previous studies of energetic stability and transient growth.

Keywords: Stability; Hartmann layers; Bödewadt layers

1. Introduction

In numerous engineering applications magnetic fields are used to drive flows, induce stirring, levitation or to suppress turbulence in electrically conducting fluids. Examples can be found in the casting of metals and the growth of semiconductor crystals [1]. In those magnetohydrodynamic (MHD) flows the balance of Lorentz and viscous forces along boundaries non-tangential to the magnetic field gives rise to Hartmann boundary layers. These layers are peculiar in the sense that they act as channels for the electric currents, determining the characteristics of the velocity in the core of the flow. Their thickness is $O(Ha^{-1}L)$, where L is a characteristic length and the Hartmann number is given by $Ha = LB\sqrt{\sigma/\rho\nu}$, with σ, ρ, ν the electrical conductivity, density and kinematic viscosity of the fluid, respectively, and B the intensity of the magnetic field. Information on the parameter ranges for which the layer is laminar or turbulent is crucial in any activity where a detailed control of the flow is required.

The velocity profile of the unperturbed two-dimensional Hartmann layer shows an exponential dependence on the distance to the boundary, similar to the asymptotic suction profile [2], and as in that case it presents a high critical Reynolds number [3]. The inclusion of the Lorentz forces term in the stability equations leaves this value almost unchanged at $R_c \approx 48250$ [4], where R is the ratio of the Reynolds to the Hartmann number, equivalent to a Reynolds number based on the thickness of the Hartmann layer. This shows that, due to the lack of inflection points in the basic flow velocity profile, the most unstable mode has a viscous origin and is a two-dimensional Tollmien–Schlichting wave in the direction of the basic flow, as implied by Squire's theorem.

From the experimental point of view, the laminarisation of magnetically driven flows in ducts of rectangular cross section was found to occur in the range $150 < R_c < 250$ [5], depending on the aspect ratio of the ducts. Lingwood and Alboussière [4] speculated that the transition observed in those flows corresponds to a laminarisation of the Hartmann layers along the walls perpendicular to the magnetic field, and that the finite-amplitude disturbances in the turbulent flow induce nonlinear effects that are responsible for the discrepancy between the critical Reynolds number for transition, as predicted by the linear stability

☆ This work was supported in part by the Engineering and Physical Sciences Research Council of the UK, grant GR/N04072.
* Corresponding author. Present address: Department of Physics and Astronomy, University of Manchester, Manchester M13 9PL.
E-mail address: pablo@reynolds.ph.man.ac.uk (P. Moresco).

0997-7546/$ – see front matter
doi:10.1016/j.euromechflu.2004.04.001

analysis, and the value measured for laminarisation. This idea received further support by the results of a weakly-nonlinear stability study which found that the Hartmann layer presents subcritical instability, i.e. small but finite-amplitude perturbations can grow for subcritical values of the Reynolds number [6]. Lingwood and Alboussière [4] used an energetic analysis [7] and found that the minimum Reynolds number for which the basic flow is able to transfer energy to a disturbance of any size is $R \approx 26$. At lower values of R all disturbances decay monotonically.

While the theoretical stability studies mentioned above focused on the isolated two-dimensional Hartmann layer, for certain configurations, like in the use of rotating magnetic fields in the metallurgical industry, or in geophysics when considering the flow in the Earth's liquid inner core, three-dimensional effects cannot be neglected. The presence of magnetic fields and the associated Lorentz forces indicates that these layers will share some of the characteristics of the Hartmann layer. Here we studied the combination of the layer that arises in a flow in solid-body rotation over a steady solid plane, generally known as Bödewadt flow, when a magnetic field perpendicular to the plane is also present. As shown by Davidson [8] this type of layers will control the swirling flow that arises in some configurations for the casting of metals.

Being part of the family of rotating flows together with the Ekman and the von Karman (rotating disk) layers, the Bödewadt layer shares many of their stability properties, and it was found by Faller [9] to be the most unstable of the three. As in the von Karman and Ekman layers, he identified two types of instabilities: spiral steady and travelling vortices, also known as type I and II instability modes, which first become amplifying at $R_c \approx 25$ and $R_c \approx 15$ respectively, with R a Reynolds number based on the thickness of the Bödewadt layer. The first type of instability is known to have an inviscid origin and to result from the inflection points in the basic velocity profile, as was proved by Gregory et al. [10] for the rotating disk flow. The second type of instability originates from the effects of viscosity and the curvature of the streamlines and presents the lowest critical Reynolds number, although its growth rate is smaller than that for type I instability. These results are in good agreement with the experiments by Savaş [11].

Far from the boundary in the Bödewadt layer, there is an equilibrium between the centrifugal forces and the axially independent radial pressure gradient, but near the solid boundary the centrifugal forces are reduced by the action of viscosity and the pressure gradient causes a predominantly inward radial flow, and to satisfy continuity, an upwards axial flow. The interplay between Coriolis and Lorentz forces in the Bödewadt–Hartmann layer was studied by King and Lewellen [12] and Davidson and Pothérat [13]. The relative importance of the two effects can be measured by the Elsasser number

$$\Lambda = \frac{B^2\sigma}{2\Omega\rho}, \tag{1}$$

where Ω is the angular velocity of the flow far from the solid boundary. The Lorentz forces will act both by modifying the basic velocity profile in the boundary layer and by damping the disturbances. Gilman [14] studied these effects in the case of the combined Ekman–Hartmann boundary layer and found that both type I and II instabilities in the Ekman layer remain for the mixed layer, but the critical Reynolds number increases with Λ, showing the stabilising effect of the magnetic field. Similar behaviour was found for the Ekman–Hartmann layer on a spherical boundary by Desjardins et al. [15] for the range of parameters relevant to the Earth's core.

In Section 2 of the paper we define the configuration and deduce the equations describing the basic flow and the linear stability problem for the Bödewadt–Hartmann layer. The numerical results of these equations for a wide range of values of Λ are presented and discussed in Section 3. In the final part of the paper especial attention is given to the high Λ regime as it can shed some light on the mechanisms that initiate transition in the two-dimensional Hartmann layer.

2. Basic flow and stability equations

We considered the ideal problem of an electrically conducting fluid rotating with uniform angular velocity over an infinite, flat plane. We assumed the fluid to be homogeneous and incompressible and to have constant physical properties, and the existence of an imposed uniform magnetic field B aligned with the axis of rotation, perpendicular to the plane.

Under the usual approximations in magnetohydrodynamics [16], and for small magnetic Reynolds numbers, i.e. assuming that the external magnetic field is unperturbed by the induced magnetic field, the flow is described by

$$\frac{\partial\tilde{\mathbf{v}}}{\partial t} + \tilde{\mathbf{v}}\cdot\nabla\tilde{\mathbf{v}} = \frac{1}{\rho}\big(\tilde{\mathbf{j}}\times\widetilde{\mathbf{B}}\big) - \frac{1}{\rho}\nabla\tilde{p} + \nu\nabla^2\tilde{\mathbf{v}}, \tag{2}$$

$$\nabla\cdot\tilde{\mathbf{v}} = 0, \tag{3}$$

$$\tilde{\mathbf{j}} = \sigma\big(-\nabla\tilde{\varphi} + \tilde{\mathbf{v}}\times\widetilde{\mathbf{B}}\big), \tag{4}$$

$$\nabla\cdot\tilde{\mathbf{j}} = 0, \tag{5}$$

where $\tilde{\mathbf{v}} = (\tilde{u}, \tilde{v}, \tilde{w})$ is the velocity vector, $\tilde{\mathbf{j}}$ is the current density vector field, $\tilde{p}$ the pressure, t the time and $\tilde{\varphi}$ the electric potential field. We adopted cylindrical polar coordinates r, θ and z, with $z = 0$ being the plane of the solid boundary, and assumed the fluid to be contained in the half-space $z > 0$.

In the steady case, axisymmetric solutions to (2)–(5) can be found of the von Karman similarity type, where $\tilde{u}$ and $\tilde{v}$ are proportional to r and $\tilde{w}$ is proportional to a length scale δ,

$$\tilde{u} = \Omega r F(z), \quad \tilde{v} = \Omega r G(z), \quad \tilde{w} = \Omega \delta H(z), \quad \tilde{p} = \rho \Omega^2 \delta^2 P(r, z), \tag{6}$$

with F, G, H and P dimensionless basic flow variables. Assuming that the wall is electrically insulating and that there are no radial currents outside the boundary layer, it can be shown [17] that the electric potential field must satisfy

$$\tilde{\varphi}(r) = \frac{B}{2} \Omega r^2. \tag{7}$$

Adopting $\sqrt{\nu/\Omega}$ and Ω^{-1} as the characteristic length and time respectively, the equations of motion reduce to

$$F^2 + HF' - G^2 + 1 - F'' + 2\Lambda F = 0, \tag{8}$$

$$2FG + HG' - G'' + 2\Lambda(G - 1) = 0, \tag{9}$$

$$2F + H' = 0, \tag{10}$$

where the primes denote differentiation with respect to z and the value of the pressure $P(r, z)$ was obtained using the azimuthal component of (2) and the fact that as $z \to \infty$ the flow is purely azimuthal and $G \to 1$, which gives

$$P(r, z) = \frac{r^2}{2} + P(z) + \text{const.} \tag{11}$$

The boundary conditions for (8)–(10) are,

$$F(0) = G(0) = H(0) = 0, \qquad F(\infty) = 0, \qquad G(\infty) = 1. \tag{12}$$

Analytical expressions for δ exist in the limits corresponding to the Bödewadt layer (δ_B) and Hartmann layer (δ_H), and both are related to the Elsasser number Λ by

$$\delta_B = \sqrt{\frac{\nu}{\Omega}} \quad \text{(Bodewadt)}, \quad \delta_H = \sqrt{\frac{\nu\rho}{\sigma B^2}} \quad \text{(Hartmann)}, \quad \frac{\delta_B^2}{\delta_H^2} = 2\Lambda. \tag{13}$$

For the Bödewadt–Hartmann layer, the value of δ for each Λ was defined numerically as the smallest value of z for which the asymptotic conditions were satisfied within two significant figures. To simplify the notation we define $\xi = \delta^2/\delta_B^2$, which as $\Lambda \to \infty$ satisfies $\xi \to 1/2\Lambda$.

A linear stability analysis was applied at a radius r_e by imposing infinitesimally small disturbances on the mean flow. In order to make the linearised equations separable in r, θ and t, it was necessary to ignore variations in the characteristic velocity with the radius. This is usually called the parallel flow approximation, although in this case the boundary layer thickness is constant, and allows for the variable r that appears in the coefficients of the linearised equations to be replaced by a local Reynolds number R. This approximation has been shown to introduce an error of $O(R^{-1})$ in the stability equations [18] and can then be expected to be valid only for $R \gg 1$. It has been found that the parallel flow approximation gives results in good agreement with experiments on rotating fluids [19,20].

The time was scaled by Ω^{-1} and the characteristic velocity, current density, pressure and local Reynolds were defined as

$$U_c = r_e \Omega, \quad j_c = \sigma U_c B, \quad p_c = U_c^2 \rho, \quad R = \frac{U_c \delta}{\nu}. \tag{14}$$

All the variables were decomposed into a mean steady part (capital letters) and a superimposed small disturbance. In nondimensional form the instantaneous nondimensional velocities, pressure and electric potential were given by

$$u^*(r, \theta, z, t) = \frac{\xi r}{R} F(z) + u(r, \theta, z, t), \tag{15}$$

$$v^*(r, \theta, z, t) = \frac{\xi r}{R} G(z) + v(r, \theta, z, t), \tag{16}$$

$$w^*(r, \theta, z, t) = \frac{\xi}{R} H(z) + w(r, \theta, z, t), \tag{17}$$

$$p^*(r, \theta, z, t) = \frac{\xi^2}{R^2} P(z) + p(r, \theta, z, t), \tag{18}$$

$$\phi^*(r, \theta, z, t) = \frac{\xi^2}{2R^2} r^2 + \phi(r, \theta, z, t). \tag{19}$$

We further assumed the perturbations to be in the form of normal modes

$$(u, v, w, p, \phi) = \big(f(z), g(z), h(z), \pi(z), \varphi(z)\big) \exp\left[\mathrm{i}\left(\alpha r + \beta \frac{R}{\xi}\theta - \omega t\right)\right], \tag{20}$$

whose real parts correspond to the physical quantities. The components of the wave vector in the radial and azimuthal directions are α and $\beta R/\xi$, and ω is the angular frequency, which is taken to be complex with real and imaginary parts ω_r and ω_i respectively. The sign of ω_i then determines if the normal mode is amplifying or decaying with time. To satisfy azimuthal periodicity, $\beta R/\xi$ has to be an integer but, as it will be seen, the values relevant to transition are much greater than 1 and R, β and ξ will be treated as real numbers. The perturbation equations were obtained by substituting (15)–(19) into the equations of motion (2)–(5) and subtracting the basic flow quantities. After linearising with respect to the perturbation variables and neglecting terms of order R^{-2} and smaller, the resulting equations are

$$\begin{aligned}&\left[\frac{1}{R}\big(D^2-\gamma^2\big)\big(D^2-\bar\gamma^2\big) + \mathrm{i}\omega\big(D^2-\bar\gamma^2\big) - \frac{2\Lambda\xi}{R}D^2 - \mathrm{i}(\alpha F+\beta G)\big(D^2-\bar\gamma^2\big)\right.\\ &\quad\left. + \mathrm{i}\big(\bar\alpha F''+\beta G''\big) - \frac{H\xi}{R}D\big(D^2-\bar\gamma^2\big) - \frac{H'\xi}{R}\big(D^2-\bar\gamma^2\big) - \frac{F\xi}{R}D^2\right]h - \left[\frac{2\mathrm{i}G\xi}{R}D + \frac{2\mathrm{i}G'\xi}{R}\right]\eta = 0,\end{aligned} \tag{21}$$

$$\left[\frac{1}{R}\big(D^2-\gamma^2\big) + \mathrm{i}\omega - \mathrm{i}(\alpha F+\beta G) - \frac{2\Lambda\xi}{R} - \frac{H\xi}{R}D - \frac{F\xi}{R}\right]\eta - \left[\alpha G' - \beta F' + \frac{2\mathrm{i}G\xi}{R}D\right]h = 0, \tag{22}$$

where D and the primes denote derivatives with respect to z and

$$\bar\alpha = \left(\alpha - \mathrm{i}\frac{\xi}{R}\right), \quad \gamma^2 = \alpha^2+\beta^2, \quad \bar\gamma^2 = \alpha\bar\alpha+\beta^2, \quad \eta = \bar\alpha g = \frac{1}{R}\left[\frac{\partial(rv)}{\partial r} - \frac{\partial u}{\partial\theta}\right],$$

i.e. η is proportional to the component of the vorticity in the $\hat z$ direction. The corresponding boundary conditions are,

$$h(0) = h'(0) = \eta(0) = 0, \qquad h(\infty) = h'(\infty) = \eta(\infty) = 0. \tag{23}$$

3. Numerical results and discussion

3.1. Neutral stability curves

The solutions of the basic flow equations (8)–(10) were obtained numerically using a shooting method with Runge–Kutta integration. In Fig. 1 are shown the three components of the velocity for different values of the Elsasser number, where the spatial coordinate z was nondimensionalised using δ_B. For $\Lambda = 0$ (Bödewadt layer) the conditions of constant angular velocity far from the boundary and decay of the tangential velocity to zero at the wall induce a radial inflow and a local overshoot of the tangential velocity. As the strength of the magnetic interaction grows (Λ increases), the oscillations in G are damped and the boundary-layer thickness decreases ($\xi \to 0$), while the azimuthal velocity profile approaches that of the Hartmann layer. The magnetic field damps the components of the vorticity perpendicular to it, and the U and W components of the velocity tend to zero with growing Λ. In Table 1 are given some values of ξ for different Λ obtained numerically as described in Section 2. Fig. 1 also reveals that the transition from the Bödewadt to the Hartmann regimes takes place within a rather small range of the Elsasser number.

The stability equations (21), (22) were solved using a spectral Tau method based on expansions in Chebyshev polynomials [21], and the solution of the resulting algebraic equations was obtained using routines from the LAPACK numerical library [22]. In Fig. 2 are shown the neutral curves ($\omega_i = 0$) of the most unstable mode also present in the Hartmann layer. This mode corresponds to two-dimensional Tollmien–Schlichting waves in the azimuthal direction ($\alpha = 0$) which become increasingly unstable when the rotational effects become more important, but its critical Reynolds number remains high even at low values of the Elsasser number ($R_c \approx 20000$ for $\Lambda = 0.5$). Fig. 3 shows the neutral curves corresponding to type I instability in the Bödewadt layer. The inviscid character of this mode makes it dependent on the presence and position of inflection points in the basic velocity profile. In the Bödewadt layer the three components of the velocity possess inflection points, resulting in a very low critical Reynolds number. With increasing Λ the inflection points become less pronounced and finally disappear from the basic flow, which is reflected in an increasing R_c. Also to be noticed is that β and the azimuthal component of the wave vector, and the angle of these stationary vortices with respect to the radius, decrease with Λ.

The effect of varying Λ on the type II instability mode of the Bödewadt layer is shown in Fig. 4, where each neutral curve corresponds to a fixed value of α, equal to that at the corresponding critical point. As shown by Faller [9], this mode is maintained by a transfer of energy from the basic flow into u through the Reynolds stresses induced by G', which is then distributed to the other components of the velocity by the centrifugal terms; i.e. this instability is due to viscosity and the

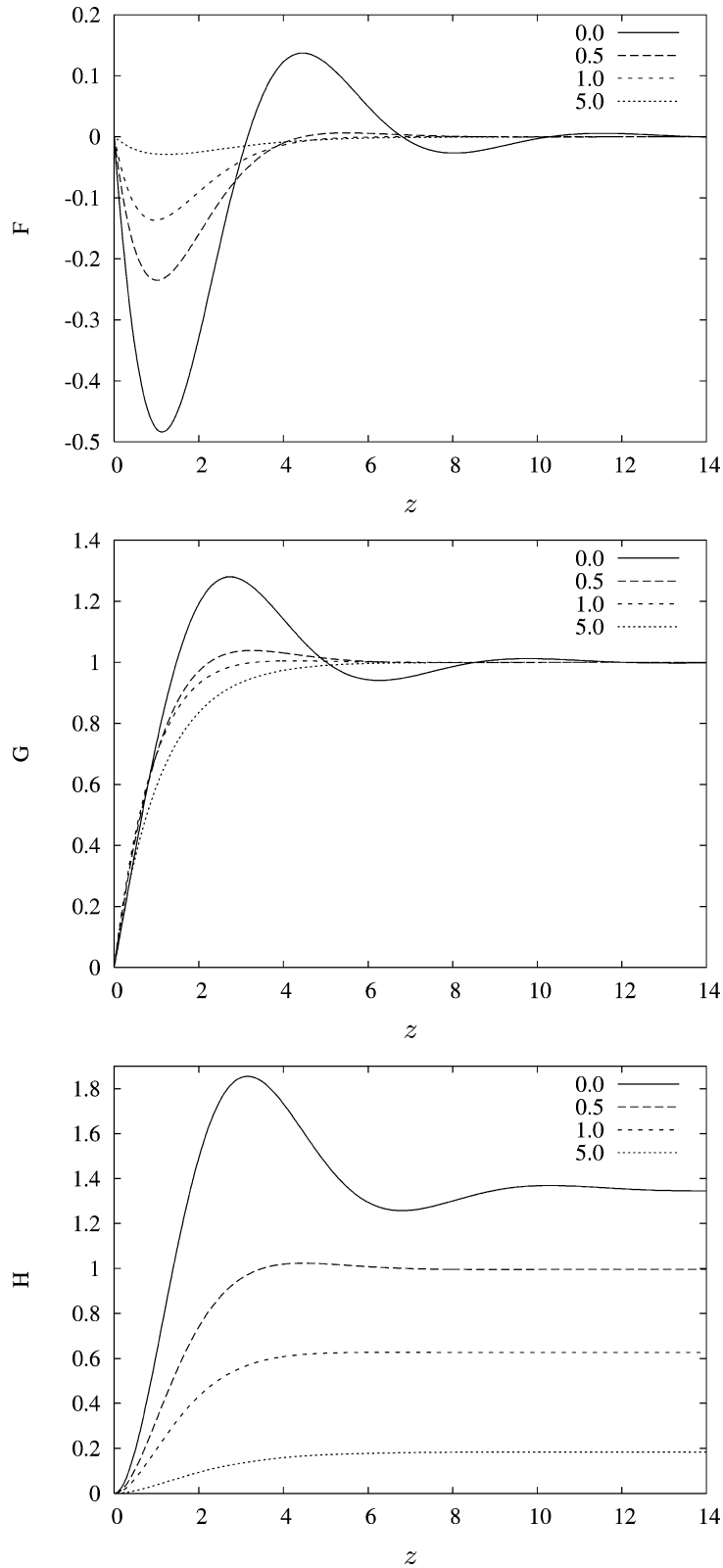

Fig. 1. Radial (F), azimuthal (G) and axial (H) components of the basic flow velocity field for different values of Λ (different line types).

Table 1
Numerical values of $\xi = \delta^2/\delta_B^2$ and critical R, α and β for different values of the Elsasser number Λ. The superscripts identify type I and II instabilities

Λ	ξ	R_c^{I}	α_c^{I}	β_c^{I}	R_c^{II}	α_c^{II}	β_c^{II}
0	1	29	0.51	0.12	21	0.3	-0.15
0.3	0.86	74	0.39	8.6×10^{-2}	63	0.29	-7.9×10^{-2}
1	0.37	247	0.30	4.2×10^{-2}	224	0.22	-1.5×10^{-2}
2	0.23	560	0.28	1.9×10^{-2}	509	0.21	-1.1×10^{-2}
5	0.08	1370	0.27	7.5×10^{-3}	1221	0.2	-2.4×10^{-3}

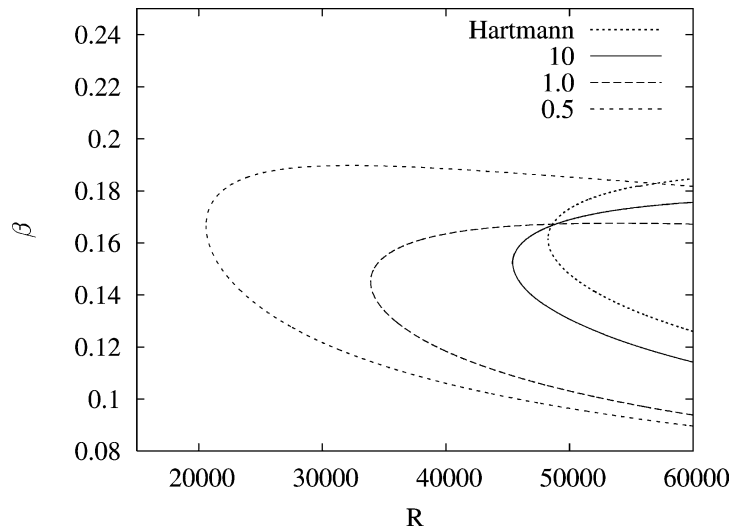

Fig. 2. Neutral curve for the Hartmann mode for different values of Λ. The curve labelled Hartmann corresponds to the two-dimensional Hartmann layer.

curvature of streamlines. Both positive and negatives values of ω_r become unstable, showing that this mode has the form of vortices travelling both upstream and downstream. This is the most unstable mode in the Bödewadt layer and remains so for $\Lambda \neq 0$. Nevertheless, its amplification rate is lower than that of the type I mode at the same R. As Λ is increased and the U and W components of the velocity tend to zero this mode becomes more stable. As with the type I instability it is found that, at high values of Λ, the azimuthal component of the wave vector and ω_r tend to zero, which means that the instability takes the form of stationary streamwise vortices. In Table 1 are given the values of R, α and β for the critical points for modes I and II and different values of Λ. The small difference with previous results for the Bödewadt layer [9] is probably due to the difference in numerical techniques.

From these results, the scenario predicted by the linear stability analysis for finite Λ consists of a laminar region near the centre of rotation (low R) surrounded by a region where type II vortices become unstable and another region where type I instability appears. As the most unstable modes are inner propagating, they will grow until they reach the stable region and they will then decay; in consequence it is to be expected that transition will occur at a higher R_c than the minimum.

3.2. High Λ limit

The stability equations (21), (22) differ from that for the purely two-dimensional Hartmann layer in the terms containing the radial (F) and axial (H) components of the velocity of the basic flow, and in the last two terms in (21) and the last term in (22), which are due to the curvature of the streamlines and are $\mathrm{O}(R^{-1})$, so they do not persist in the inviscid limit at large r_e. In the limit $\Lambda \to \infty$, the basic flow in the azimuthal direction approaches the Hartmann layer profile and it can be seen from (8)–(10) that $(G-1)$, F and H are $\mathrm{o}(2^{-1}\Lambda^{-1})$; so in the stability equations only the $\mathrm{O}(2^{-1}\Lambda^{-1})$ streamline curvature terms persist. At high Λ the addition of these terms can be thought as a small perturbation to the stability problem for the purely two-dimensional Hartmann layer and our stability calculations show that they are responsible for the type II instability mode, which presents a much lower critical R than the Hartmann mode, even for large Λ.

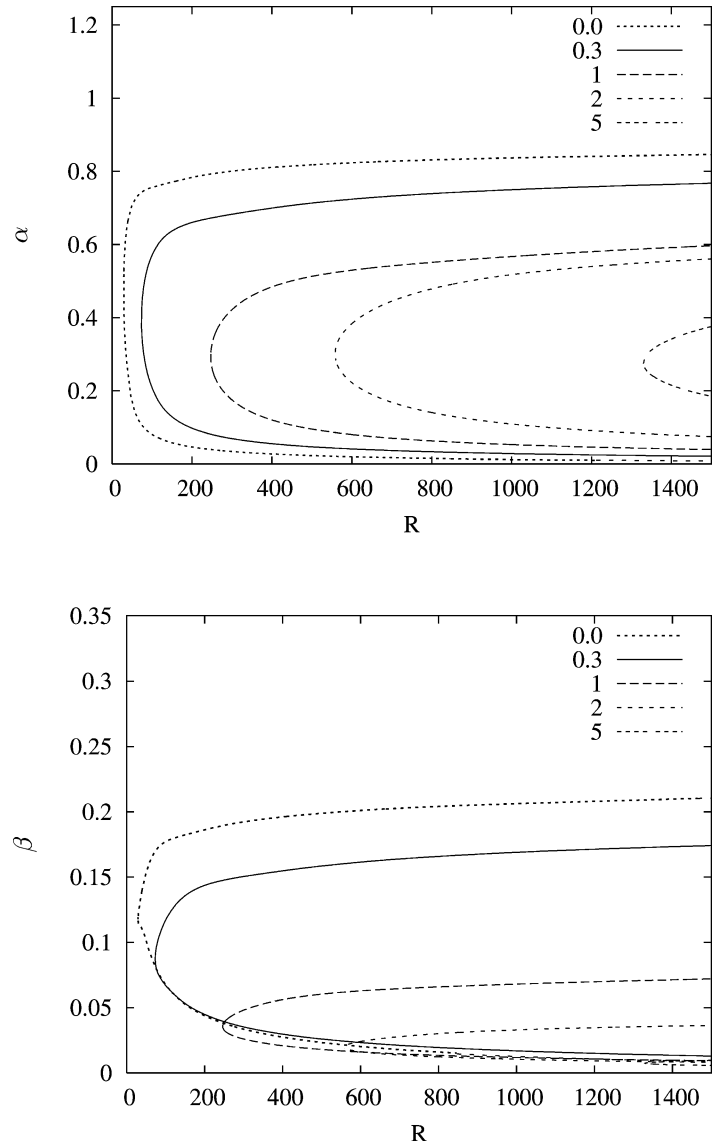

Fig. 3. Neutral curve of the type I instability mode for different values of Λ.

It is known in hydrodynamic stability theory that systems that are highly sensitive to perturbations of the basic flow can sustain growing disturbances in subcritical regions of parameter space [23]. Although this growth is transient and algebraic instead of exponential, the disturbances can reach considerable size and trigger nonlinear effects. This mechanism was first identified by Ellingsen and Palm [24] and Landahl [25], and is due to the non-normality of the linear stability operator and the fact that the associated eigenfunctions are nearly linearly dependent. Gerard-Varet [26] showed this to be the case for the Hartmann layer flow, where perturbations can be amplified by a factor of 23 for R as low as 200. He also found that the optimal perturbations, i.e. those experiencing the highest amplification rate, are stationary streamwise vortices, which are also the perturbations that can achieve the highest transfer of energy from the basic flow [4]. Another way of understanding the same phenomenon is that the solutions presenting transient growth correspond to unstable solutions of an stability problem that differs from the original one in a small perturbation, due for example to changes in the basic velocity profile or the presence of noise. If the linear stability operator is highly non-normal the perturbed flow can have stability properties that are substantially different from the original problem. The findings in this paper show a physical configuration where this happens, as the addition of small rotational effects to the Hartmann layer reduces the critical Reynolds number by an order of magnitude and gives rise to unstable modes in the form of structures approximately aligned in the flow direction, in agreement with Gerard-Varet's work.

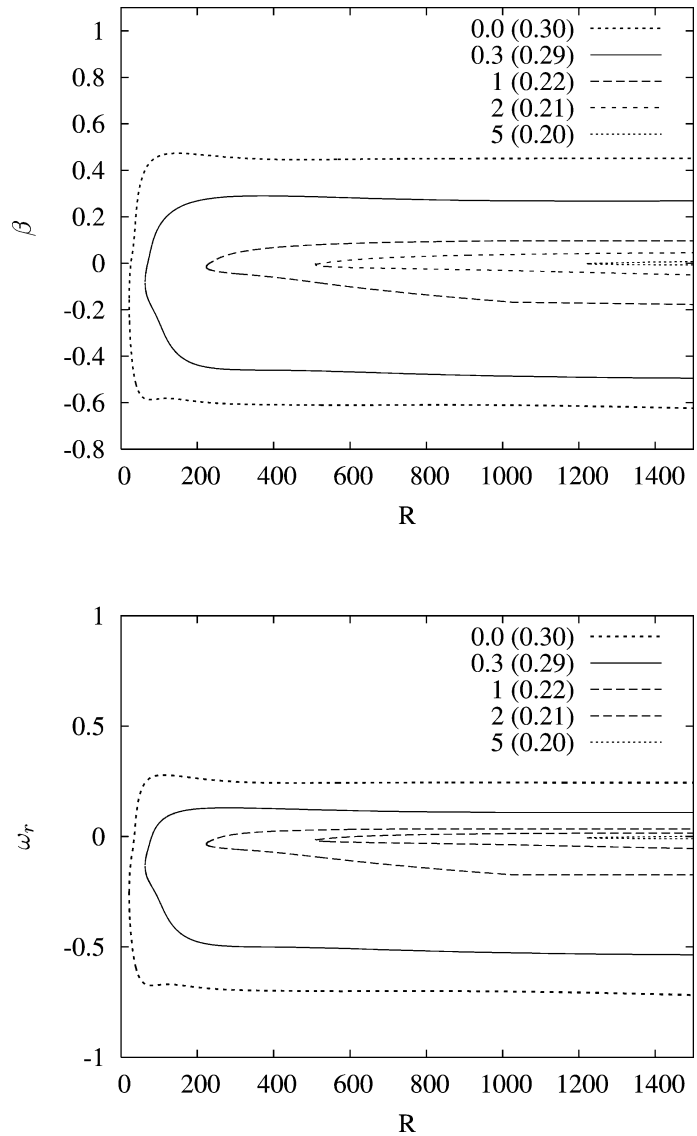

Fig. 4. Neutral curve of the type II instability for different values of Λ and for the values of α at the critical points (indicated between brackets).

The linear stability analysis presented above shows that in the Bödewadt–Hartmann layer rotational effects are crucial in determining the stability of the flow, even when electromagnetic effects are dominant ($\Lambda > 1$). The most destabilising influence is given by a combination of viscosity and the curvature of the streamlines, with a critical Reynolds number that differs by more than one order of magnitude from that of the most unstable purely viscous mode. This suggests that in practical and natural conditions where three-dimensional effects will be present most of the time, although their origin might be different from rotation, the transition to turbulence in the Hartmann layer, as well as its laminarisation, will occur at values of R well below the critical according to the linear stability theory.

References

[1] J.P. Garandet, T. Alboussière, Bridgman growth: modelling and experiments, Prog. Crystal Growth and Charact. 38 (1999) 73–132.
[2] H. Schlichting, Boundary Layer Theory, McGraw-Hill, New York, 1960.
[3] R.C. Lock, The stability of the flow of an electrically conducting fluid between parallel planes under a transverse magnetic field, Proc. Roy. Soc. London Ser. A 233 (1955) 105–125.

[4] R.J. Lingwood, T. Alboussière, On the stability of the Hartmann layer, Phys. Fluids 8 (1999) 2058–2068.
[5] G.G. Branover, Resistance of magnetohydrodynamic channels, Magnetohydrodynamics 3 (1967) 1–11.
[6] P. Moresco, T. Alboussière, Weakly nonlinear stability of Hartmann boundary layers, Eur. J. Mech. B Fluids 22 (2003) 345–353.
[7] D.D. Joseph, Stability of Fluid Motions, Springer, New York, 1976.
[8] P.A. Davidson, Swirling flow in an axisymetric cavity of arbitrary profile, driven by a rotating magnetic field, J. Fluid Mech. 245 (1992) 669–699.
[9] A.J. Faller, Instability and transition of disturbed flow over a rotating disk, J. Fluid Mech. 230 (1991) 245–269.
[10] N. Gregory, J.T. Stuart, W.S. Walker, On the stability of three-dimensional boundary layers with the application to the flow due to a rotating disk, Philos. Trans. Roy. Soc. London Ser. A 248 (1955) 155–199.
[11] Ö. Savaş, Stability of Bödewadt flow, J. Fluid Mech. 183 (1987) 77–94.
[12] W.S. King, W.S. Lewellen, Boundary-layer similarity solutions for rotating flows with and without magnetic interaction, Phys. Fluids 7 (1964) 1674–1680.
[13] P.A. Davidson, A. Pothérat, A note on Bödewadt–Hartmann layers, Eur. J. Mech. B Fluids 21 (2002) 545–559.
[14] P.A. Gilman, Instabilities of the Ekman–Hartmann boundary layer, Phys. Fluids 14 (1971) 7–12.
[15] B. Desjardins, E. Dormy, E. Grenier, Instability of Ekman–Hartmann boundary layers, with application to the fluid flow near the core-mantle boundary, Phys. Earth Planet. Interiors 123 (2001) 15–26.
[16] J.A. Shercliff, A Textbook of Magnetohydrodynamics, Pergamon Press, 1965.
[17] C.J. Stephenson, Magnetohydrodynamic flow between rotating coaxial disks, J. Fluid Mech. 38 (1969) 335–352.
[18] P.R. Spalart, Direct numerical study of crossflow instability, in: D. Arnal, R. Michel (Eds.), Laminar-Turbulent Transition, Springer, 1990.
[19] R.J. Lingwood, Absolute instability of the boundary layer on a rotating disk, J. Fluid Mech. 299 (1995) 17–33.
[20] R.J. Lingwood, An experimental study of absolute instability of the rotating-disk boundary-layer flow, J. Fluid Mech. 314 (1996) 373–405.
[21] C. Canuto, M.Y. Hussaini, A. Quarteroni, T.A. Zang, Spectral Methods in Fluid Dynamics, Springer-Verlag, Berlin, 1988.
[22] E. Anderson, Z. Bai, C. Bischof, J. Demmel, J.J. Dongarra, J. Du Croz, A. Greenbaum, S. Hammarling, A. McKenney, S. Ostrouchov, D. Sorensen, LAPACK Users' Guide, second ed., SIAM, 1995.
[23] L.N. Trefethen, A.E. Trefethen, S.C. Reddy, T.A. Driscoll, Hydrodynamic stability without eigenvalues, Science 261 (1993) 578–584.
[24] T. Ellingsen, E. Palm, Stability of linear flow, Phys. Fluids 18 (1975).
[25] M.T. Landahl, A note on an algebraic instability of inviscid parallel shear flows, J. Fluid Mech. 98 (1980) 243–251.
[26] D. Gerard-Varet, Amplification of small perturbations in a Hartmann layer, Phys. Fluids 14 (2002) 1458–1467.